

Astronomy 155: Introduction to Observational Astronomy

November 27, 2023

Lab Report 5

Lab 5: Stellar Spectroscopy

Elko Gerville-Reache

Lab mates: Isabel Shim

Introduction:

Spectroscopy revolutionized astronomy, as it allowed astronomers to probe distant astronomical objects' compositions. Stars emit blackbody radiation, characterized by an almost continuous spectrum of light, discontinuous only from emission and absorption lines. These lines indicate the chemical composition of the astronomical body. Photons produced by a star approximately originate from the center, and must travel through the star's layers before it is emitted and can be detected. These photons pass through the star's layers, which contain different molecular compositions, and when a photon with the right energy level, and hence wavelength interacts with the right molecule, that energy will be transferred to an electron. The electron is excited to a higher energy level by absorbing that wavelength, which corresponds to an absorption line in the stars' spectrum. Over time, the electron will gradually de-excite to lower energy levels, and each time will emit a photon at a lower energy level (hence the name emission lines) until the electron is back to its ground state, therefore conserving energy. Thus, a star's spectrum will contain absorption and emission lines from this process, with the emission lines typically located at lower energies (higher wavelengths). This can be imaged by separating the stars' light into its spectral components using a grating or prism and focusing it onto a CCD.

Stars are characterized by the spectral type, which corresponds to the star's temperature. In 1912, Deaf astronomer Annie Jump Cannon finalized what is the first modern stellar classification system, now known as the Harvard Classification System. Stars are grouped into 7, classes: O, B, A, F, G, K, and M, each with additional subclasses 0-9 ranging from hotter to cooler¹. In this lab, we focused on imaging 3 different stars of different spectral ranges to demonstrate the effect temperature has on the spectra of a star. For the lab, a hot (O-A), sun-like (F-G), and cool (K-M) star were chosen and imaged using a spectrograph. For the hot star, Deneb (A2Ia) was chosen, with an apparent magnitude of +1.25 and a J2000 RA, DEC of 22h30m29.26s, +43°07'24.1". Sun-like star Sadr (F8Ib) was chosen, with an apparent magnitude of +2.20 and an RA, DEC of 20h22m13.71s, +40°15'24.0". The cool star 53 Cygni (K0III) was chosen with an apparent magnitude of +2.45, and an RA, DEC of 20h46m13.35s, +33°58'21.1". All three stars are located in the constellation of Cygnus and are visually bright to the naked eye.

Observations:

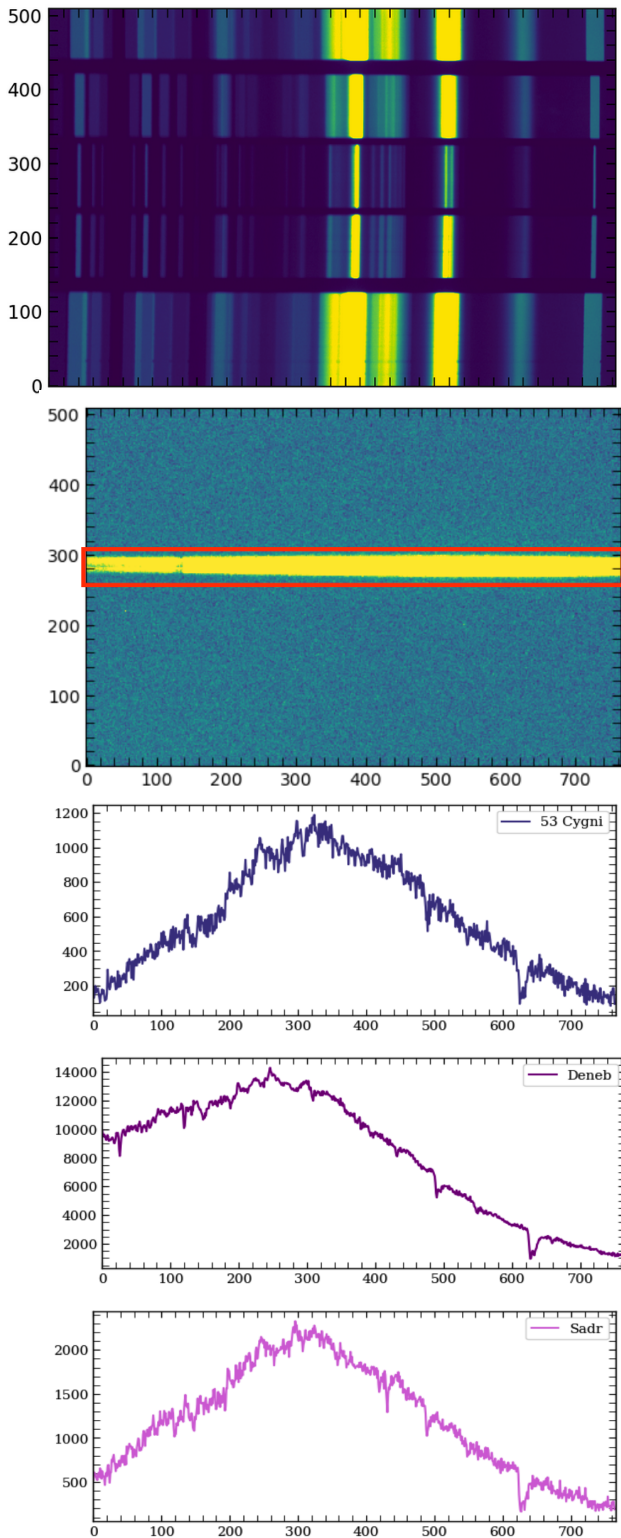
Observations were conducted at the New Haven Leitner Family Observatory and Planetarium (LFOP) on November 1, at EST: 10:00 pm with clear skies and decent seeing. The main telescope used was a 16" f/8.9 RCOS ritchey-chretien mounted on a guided equatorial mount to account for Earth's rotation. An SBIG DSS7 spectrograph mounted to an ST402ME CCD was used to collect the data. The spectrograph operates in two modes: 'position mode' and grab 'spectrum.' The former tilts the grating to act as a mirror allowing you to see the field of view of the telescope, and position the target. The latter puts the slit into place and tilts the grating into first order, thus focusing the first-order spectrum onto the CCD. The telescope is operated via a computer interface with an integrated star atlas, allowing for easy slewing and centering of objects. The program also controls the camera focus, shutter speed, and binning. At the time of observation, the constellation Cygnus was high in the sky, and the proximity of all three targets made observations easy, as displayed in Figure 1. For each target, three, 1" long exposures were taken, along with three darks. The darks were taken by taking a spectrum of a blank patch of sky in the vicinity of the target stars. Three calibration

spectra were also taken of a mercury light bulb for calibrating the wavelengths. Mercury has known emission lines, known to a high precision from lab tests and these lines will be used later to calibrate the spectra of the target stars.



Figure 1: Sample star chart of the three target stars in Cygnus, courtesy of stellarium².

Data Analysis and Reduction:



All raw fits files were loaded into Python and reduced using the standard astronomical reduction pipeline. All dark frames were median combined into a master dark file and subsequently subtracted from each light frame, including the mercury spectrum. Doing so accomplishes two goals: dark subtraction greatly increases the signal-to-noise ratio but since the dark frames are comprised of a blank sky spectrum, sky subtraction is also achieved. After dark subtraction, all corresponding light frames were median combined into reduced light frames. After calibration, we are left with a median combined light frame for each star, as well as a reduced mercury spectrum. The images were left unregistered for this reduction as aligning the spectra is not necessary. After an initial reduction step, the images are cropped to contain only the data, as demonstrated in figure 3 by the red box. The cropped image represents a 1-dimensional image that contains the spectrum. Summing along the zeroth axis in python creates a matrix of intensities that represents our raw spectrum. The image is now ‘flattened’ and can be plotted to visualize the uncalibrated spectrum, as shown in figure 4. Already, there are lots of noticeable absorption lines present in the continuum of the spectra. Each one of these dips is a signature from some element or molecule found in the star. The axes are unlabeled as the wavelengths (x-axis) and flux (y-axis) are yet to be calibrated and only represent relative units.

Figures 2,3,4: Figure 2 (topmost) shows the fully reduced mercury spectrum. The vertical colored lines represent the mercury emission lines from the bulb. Figure 3 (middle) shows the uncoded Sadr spectrum while figure 4 shows the uncalibrated spectra of 53 Cygni, Deneb, and Sadr.

To identify the absorption lines in the spectra, wavelength calibration is required. To do so, the mercury image was cropped and flattened similarly to the star images, and a raw spectrum was produced (figure 5):

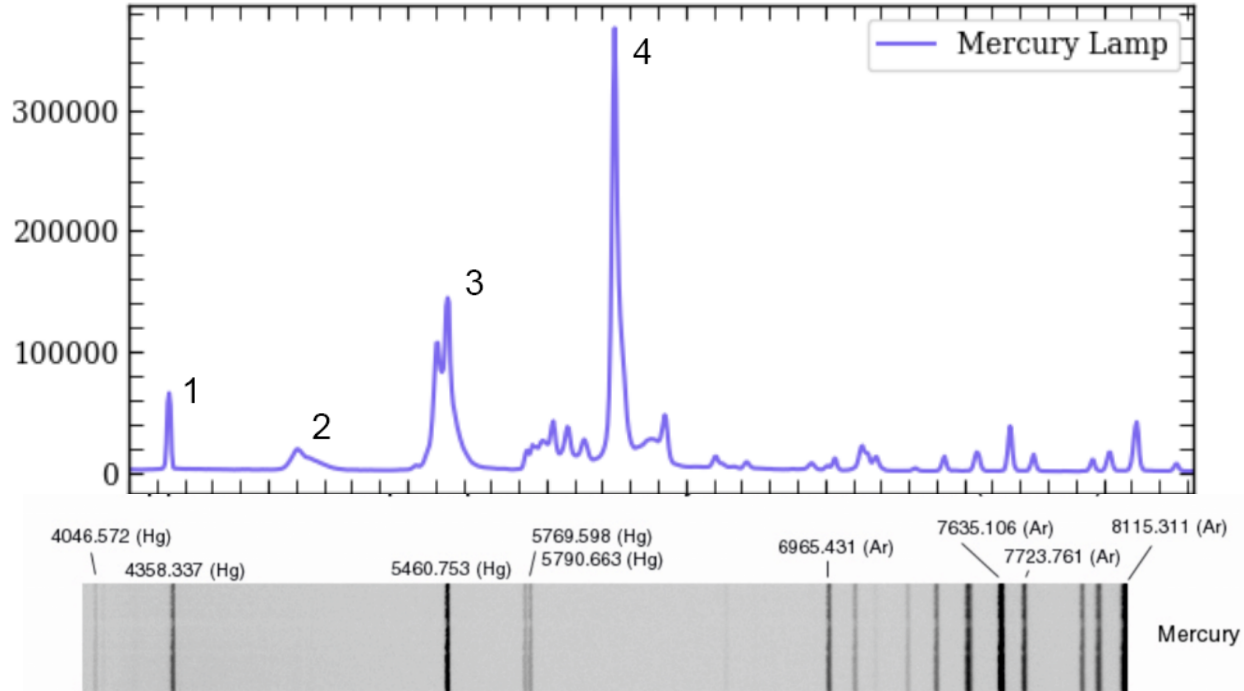


Figure 5,6: Figure 5 (topmost) shows the raw intensity plot of the mercury lamp along with its emission lines (pointing up rather than down for absorption lines). Figure 6 (bottom) shows the emission wavelengths of mercury, reproduced from the DSS7 manual³.

Using the wavelength chart (figure 6), the lines in the spectrum numbered 1-4 (figure 5) were determined to correspond to wavelengths 404.6, 407.8, 435.8, and 546.1 nanometers. These peaks correspond to x-axis pixel values of 37.0, 117, 222.6, 346.2. Using the python function `np.polyfit`, a linear regression was computed to convert pixel values to wavelengths, displayed in figure 7. This is then used to scale the wavelengths

in the stellar spectra. An array the size of the x-dimension of the spectra is created, in this case equally spaced numbers from 0 to 765. This is then scaled using the regression to become a new array containing the calibrated wavelengths.

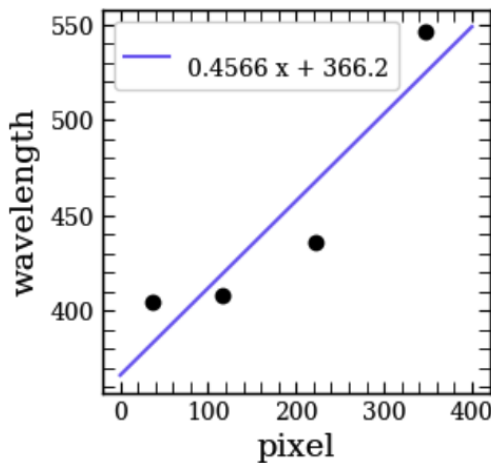


Figure 7: plot of pixels v. wavelengths and corresponding regression.

With the array containing calibrated wavelengths, we can now make plots of wavelength v. intensity, where the spectra intensities correspond to known wavelengths. This allows for the identification of absorption lines in the spectrum. The plots on the left show the intensities plotted against wavelength.

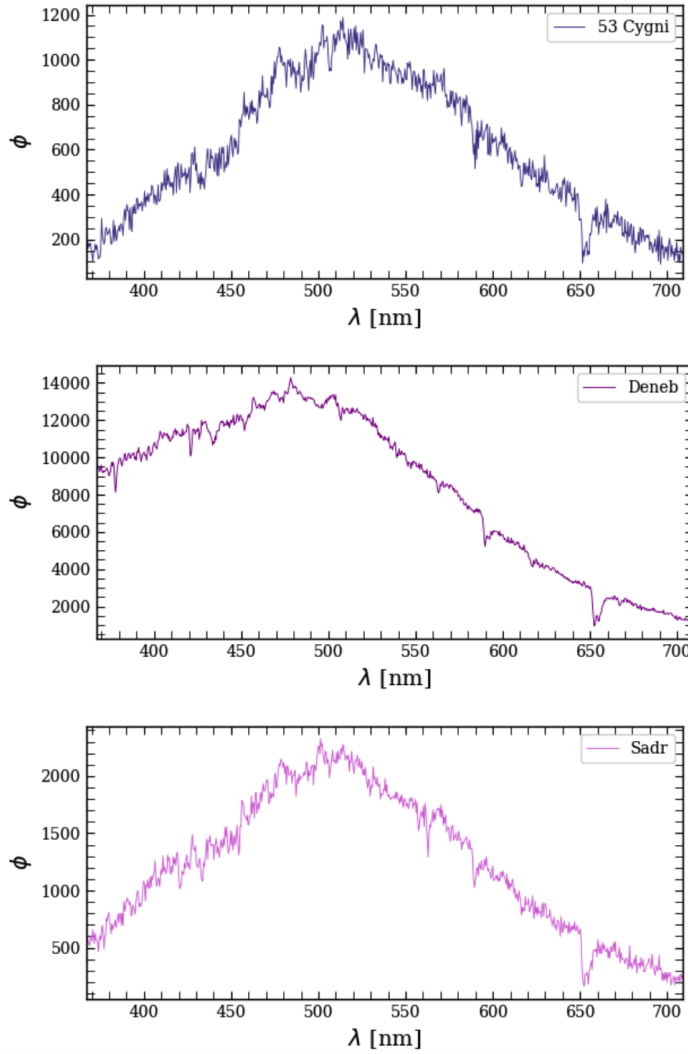


Table 1: Common Absorption Lines in Stellar Spectra
"Fr." = "Franhofer", i.e., strong lines in the solar spectrum

Line	Wavelength [Angstroms]
Fr. A band (Earth - O ₂)	7594
Fr. B band (Earth - O ₂)	6867
H-alpha	6563
Fr. D ₁ , Sodium	5896
Fr. D ₂ , Sodium	5890
Fr. E, Iron	5270
Magnesium	5184
Fr. c, Iron	4958
H-beta	4861
Fr. d, Iron	4668
Fr. e, Iron	4384
H-gamma	4340
Fr. g, Calcium	4227
H-delta	4102
Helium	4026
Helium	4009
Fr. H, Calcium	3968
H-epsilon	3967
Fr. K, Calcium	3934
H-zeta	3887
H-eta	3834
H-theta	3795
H-iota	3768

The overall shape of the continuum is unchanged compared to the plots in figure 4, yet comparing the x-axis reveals the differences. The original intensity plots ranged from 0 to 765, while the wavelength v. intensity plots in figure 8 have intensities corresponding to wavelengths. The plots have thus been rescaled using the known emission lines from the mercury lamp. The x-axis is now in units of nanometers, while the y-axis is still a relative, unitless flux, labeled Φ . For each star, the absorption lines, which are now associated with a wavelength are compared to known element emission wavelengths, shown in figure 9.

Figure 8: calibrated wavelength v intensity plots of each star. The prominent H_α line is seen at roughly 650 nanometers.

Figure 9: common absorption lines found in stellar spectra used to identify lines, courtesy of Dr. Faison.

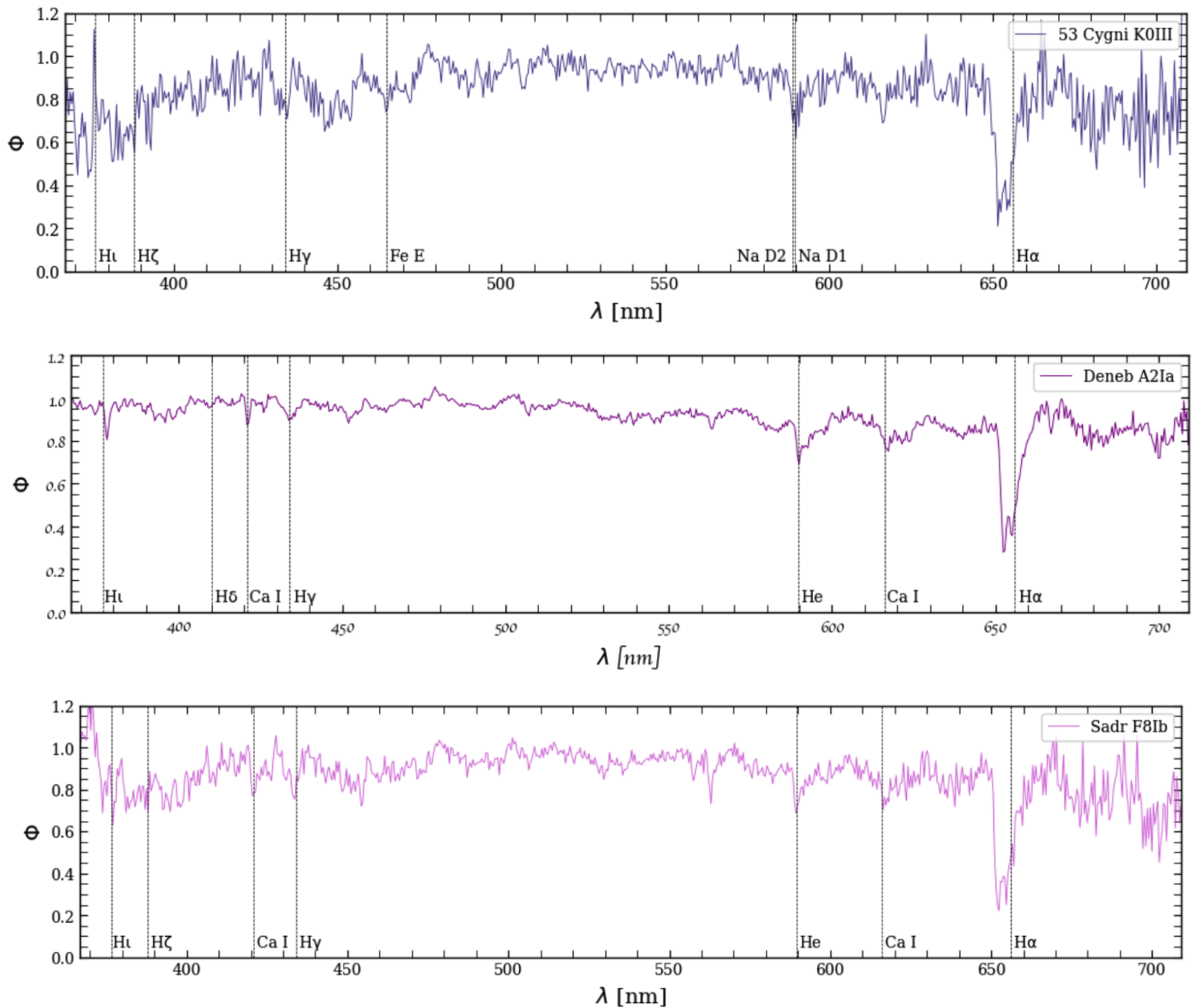


Figure 10: Finalized wavelength v. intensity plots for 53 Cygni, Deneb, and Sadr, along with identified lines.

Results:

The absorption lines (figure 10) were identified by overplotting vertical lines in python at specific wavelengths corresponding to known molecular lines⁵. This was repeated until a line matched an absorption line. The table below (figure 11) shows common spectral lines for each stellar spectral type. This was further used to discriminate which lines to fit for each star. The spectral lines found in each star made sense: 53 Cygni (K0III) had evidence of Sodium (Na, neutral metal) as well as a weak hydrogen line H ζ . Deneb (A2Ia) showed many hydrogen lines from the Balmer series (H δ , H γ , and H α), as well as He and Ca I. Sadr showed similar lines as Deneb, as F-type and A-type stars are similar in absorption lines. All three stars showed a massive H α absorption line of similar magnitude, which for Deneb and Sadr makes sense having strong H lines. The inclusion of H α in 53 Cygni is possibly from the fact that the constellation Cygnus lies in the North American Nebula, which is a massive HII region. This region most likely contaminated the spectra of all three stars, explaining the H α line present in all three spectra. The spectra absorption lines also lined up well with the expected wavelengths, especially when considering line broadening, and the combined effects of Earth's, and the stars' rotation. Figure 12 shows all lines overplotted and scaled on the y-axis for clarity. The lines match up well between the three stars showing a successful calibration and reduction of the spectra.

Spectral Class	Intrinsic Color	Temperature (K)	Prominent Absorption Lines
O	Blue	41,000	He+, O++, N++, Si++, He, H
B	Blue	31,000	He, H, O+, C+, N+, Si+
A	Blue-white	9,500	H(strongest), Ca+, Mg+, Fe+
F	White	7,240	H(weaker), Ca+, ionized metals
G	Yellow-white	5,920	H(weaker), Ca+, ionized & neutral metal
K	Orange	5,300	Ca+(strongest), neutral metals strong, H(weak)
M	Red	3,850	Strong neutral atoms, TiO

Figure 11: table demonstrating common absorption lines found in each stellar spectral type, courtesy of hyperphysics⁴.

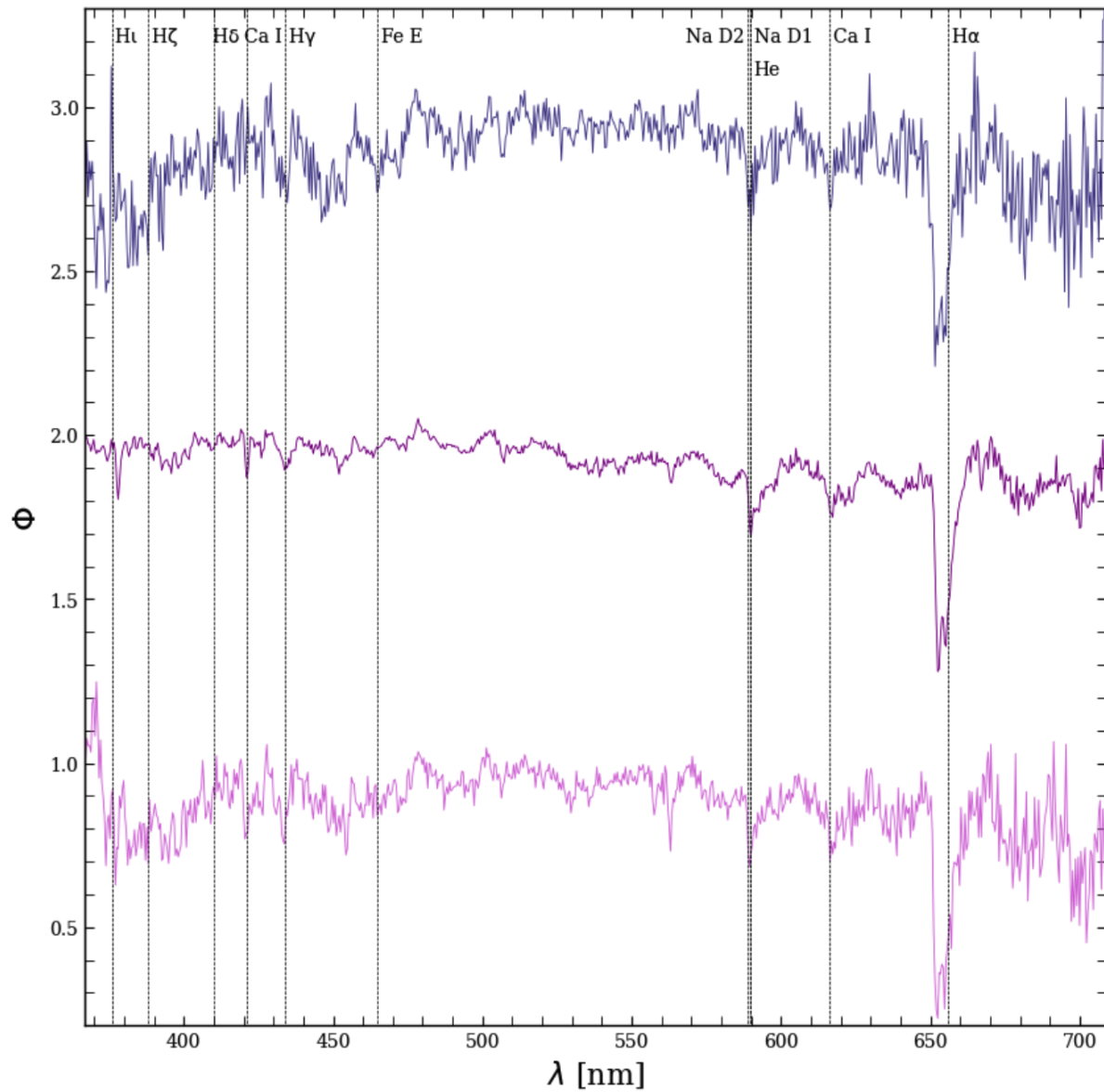


Figure 12: All three spectra overplotted for feature comparisons

References:

- 1) https://en.wikipedia.org/wiki/Stellar_classification
- 2) <https://stellarium.org/>
- 3) <https://www.dropbox.com/s/c0z146jdt4eopr/SBIG-DSS7-Manual.pdf?dl=0>
- 4) <http://hyperphysics.phy-astr.gsu.edu/hbase/Starlog/staspe.html>
- 5) <https://physics.nist.gov/PhysRefData/Handbook/Tables/sodiumtable2.htm>